20th Australasian Fluid Mechanics Conference
Perth, Australia
5-8 December 2016

Energy Dissipation rate parameter in a rough wall turbulent boundary layer

L. Djenidi[1], Md. Kamruzzaman[1] and R.A. Antonia[1]

[1]Discipline of Mechanical Engineering
The University of Newcastle, NSW 2308, Australia

Abstract

The dimensionless mean energy dissipation rate parameter C_ε is measured in a fully rough wall turbulent boundary layer at several Reynolds numbers using hot-wire anemometry. The study aims to determine the dependence of $C_\varepsilon = \bar{\varepsilon}L/u'^3$ on the distance from the wall and the Reynolds number. The results shows that C_ε decreases as the distance from the wall increases and reaches a minimum value, which appears to be independent of the Reynolds number. Further, this value, which is about 0.4-0.5, is the same as in homogeneous isotropic turbulence at high Reynolds numbers. This lends support to the possibility that a universal value for C_ε at large Reynolds numbers cannot be ruled out.

Introduction

It is believed that the constancy $C_\varepsilon = \bar{\varepsilon}L/u'^3$ ($\bar{\varepsilon}$, L and u' are the mean turbulent kinetic energy dissipation rate, the integral length scale and the rms of the longitudinal velocity) is a cornerstone assumption of turbulence theory, *e.g.* [17, 18, 11]; see also [10] for a brief review. It is often interpreted as the transfer of energy from larger to smaller scales of motion ([17, 18]). It has recently received significant attention (*e.g.* [18, 11]). The attention is mainly in determining whether the value of C_ε is universal or not at sufficiently large Reynolds number. There is in that regard no consensus yet. For example [18] argues that C_ε is a function of the Reynolds number in what he calls non-equilibrium decaying turbulent flows. He further states that C_ε is dependent of the the initial conditions and proposes the following expression $C_\varepsilon = Re_I^m/Re_L^n$, with $m \simeq 1 \simeq n$, Re_I is a global/inlet Reynolds number and Re_L a local turbulence Reynolds number. On the other hand, [10, 11] argue that C_ε reaches a universal constant of about 0.5 for isotropy and homogeneous turbulence (HIT) as the Reynolds number (*e.g.* Re_L) reaches large values. This supports the results of [13, 9] who also found that C_ε approaches a constant of about 0.5 when the Reynolds number increases, which is consistent with the findings of [5] who established lower and upper bounds for C_ε.

However, with a few exceptions (see [13, 1]) most of the attention has focused on free shear flows and decaying and forced HIT. Only a few studies report C_ε in wall bounded flows (e.g.[2, 3]). For example, [1] report C_ε across a smooth wall turbulent channel flow. They found that C_ε is about 2 and 1 in the logarithmic and outer regions, respectively. The present work is an attempt aimed at closing this gap. The main focus of this study is to assess the dependence of C_ε on the distance from the wall and the Reynolds number in a wall shear flow.

Experimental Set up

The experiments are carried out in an open wind tunnel with a test section 5.4m long and 0.15m high and 0.9m width, which follows a contraction (6:1). The top wall wall is adjusted in order to compensate for the growth of the boundary layers and to maintain a zero-pressure gradient across the entire working section of the wind tunnel. The boundary layer studied here developes on the bottom wall. It is tripped at the contraction exit by a $4-mm$-diameter rod followed by $170-mm$-long strip of No. 40 grit sandpaper. We use a rod and a sandpaper grit to trip the turbulent boundary layer, respectively, stimulating the large- and the small-scale motions in the flow. It was verified by [2] that the boundary layer produced by this type of tripping behaved according to the criteria for fully developed turbulent boundary layers. The rough wall consisted of cylindrical copper-coated rods mounted on the wall and spanning across the full width of the test section. The diameter of the rods is 1.6 mm, and the ratio λ/k is set at 8 (λ is the pitch between two consecutive rods and k is the diameter rod). This surface is identical to that used in previous studies (*e.g.* [14]) where further details can be found. The pressure gradient is maintained to within 0.1% of the free stream dynamic pressure in the working section between 1.5 and 3.1m, by adjusting the vertical wall.

Velocity measurements are made with a single hot-wire probe. The wire (diameter $d = 2.5\mu m$ and length $l = 200d$) is etched from a coil of Pt10Rh alloy. The hot wire is operated using an in-house constant temperature anemometer (hereafter, CTA) at an overheat ratio of 1.5. The output signal from the CTA circuits is amplified, offset, and low-pass filtered at a cutoff frequency (f_c) of $12,000Hz$. The sampling frequency is set at approximately $2f_c$. The hot-wire signals are digitized into a PC with a $\pm 10V$ and a 16-bit AD converter. As well as the velocity, the temperature is continuously measured in the free stream for the entire duration of the experiment using a BAT-10 thermocouple from Physitemp, USA, with a resolution of 0.1^oC. The hot wire is calibrated in situ against the Pitot-static tube positioned in the free stream before and after every experiment at 12 different speeds ranging between 0 and $16ms^{-1}$. Measurements are taken at the midpoint between consecutive roughness elements at a streamwise location x= 2.54m with the free stream velocity U_1 in the range from 10 to $16ms^1$.

The friction velocity U_τ is obtained by integrating the pressure distribution around the roughness element. For this, one of the roughness elements is replaced by a hollow cylindrical rod of identical diameter with a small circular hole drilled on its surface. The hole has a diameter of 0.3mm and acts as a static pressure tap. One end of the hollow cylindrical rod is closed, and the static pressure is measured via the other end. By rotating the tube through 2π radians, we obtain the pressure distribution around the circumference of the roughness element (for full details see [8]). The Karman number, $Re_\tau = \delta U_\tau/\nu$ (where ν is the kinematic viscosity) ranges between 620 and 7200. In both smooth and rough wall experiments, a total of 36 logarithmically spaced measurement points between 0.2 mm and 136 mm are taken at each streamwise location using the Mitutoyo height gauge with a resolution of 0.01 mm. Throughout this paper, x and y refer to the streamwise and wall-normal directions while u denotes the streamwise fluctuating velocity component.

Results

Figure 1 shows the mean velocity distribution U^+ (the superscript + represents normalization by U_τ; the distance to the wall y is normalized by δ) for several Reynolds numbers, $Re_\theta = \theta U_\tau/\nu$, ranging from about 6950 to 12650 (θ is the momentum thickness). Except for the lowest Re_θ, the profiles collapse very well across the entire boundary layer thickness. The collapse shows that the friction coefficient, C_f is independent of the Reynolds number since the value of U^+ at $y/\delta = 1$ is equal to $\sqrt{2/C_f}$. This is consistent not only with a fully rough regime (where the drag is principally due to the form drag) but also with a well approximated self-preservation state of the turbulent boundary layer over this particular rough wall as reported by [16] who also showed that U_τ was constant along x for a given Reynolds number. They argued that the roughness elements acted in such a way as to diminish significantly, if not remove, the viscosity effects across the entire boundary layer which is consistent with the fact a Reynolds number independent C_f; The dampening of the viscosity effects in the near-wall region by the roughness is reflected by the disappearance of the near-wall peak in the distribution of the u' (Figure 2) and suggests that local isotropy is likely to be better approached on the rough wall than on the smooth wall. This is important in the context of obtaining $\bar{\varepsilon}$ since it would justify the use of $\bar{\varepsilon}_{iso} = 15\nu\overline{(\partial u/\partial x)^2}$ as a surrogate for $\bar{\varepsilon}$.

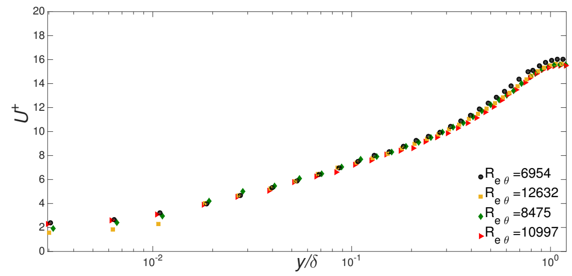

Figure 1: Mean velocity profiles U^+ for several Re_θ.

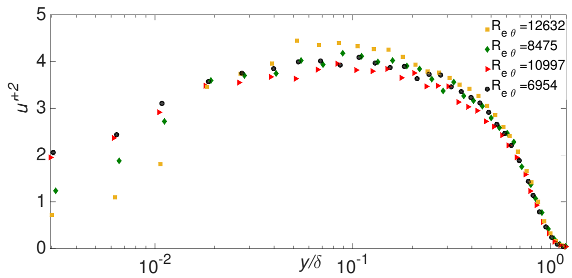

Figure 2: Profiles of u'^{+2} for several Re_θ.

An interesting feature of a turbulent boundary layer over a rough wall is that the Taylor microscale Reynolds number, Re_λ is higher than that in smooth wall turbulent boundary layer at the samie Re_θ. Figure 3 shows distributions of Re_λ across the rough wall turbulent boundary layer at $Re_\theta = 8500$ and 12600. Taylor's hypothesis of frozen turbulence has been used to convert a temporal derivative to a spatial derivative using a convection velocity equal to that of the local mean velocity. Re_λ increases rapidly with the distance from the wall, then reaches a plateau with a value of about 300 and 370 for $Re_\theta = 8500$ and 12600, respectively. The plateau extends from $y/\delta \simeq 0.2$ to about 0.6. Beyond this region Re_λ decreases. The constancy of Re_λ suggests that there exists a relatively non-negligible part ($\sim 40\%$) of the boundary layer in which the small-scale motions may be in an energy equilibrium. Further, the relatively high value of Re_λ provides confidence in the use of $\bar{\varepsilon}_{iso}$. In fact, using the spectral chart of [4] in the region away from the wall, where local isotropy is not reliable, we found that $\bar{\varepsilon}_{iso}$ underestimates $\bar{\varepsilon}$ by about 14%.

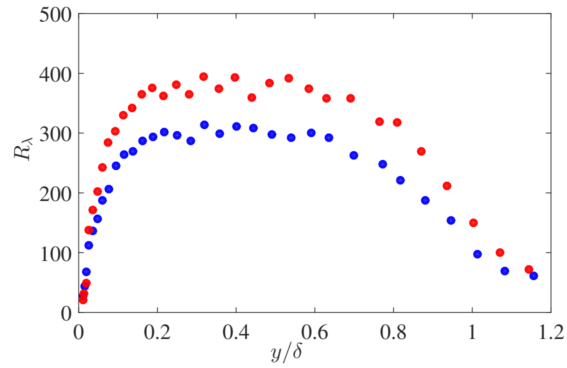

Figure 3: Distributions of Re_λ as function of y/δ at $Re_\theta = 8500$ (bleu symbols) and 12600 (red symbols).

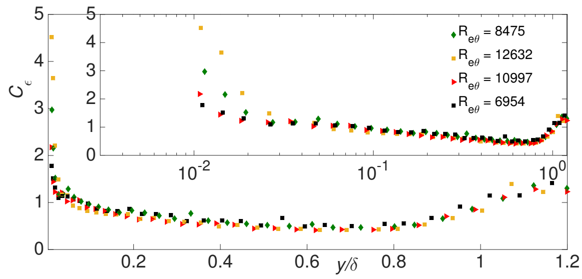

Figure 4: Distribution of C_ε as function of y/δ for various Re_θ. A semi-log scale is used in the inset to highlight the near-wall region.

The distributions of C_ε for several Re_θ are reported in Figure 4. As the distance from the wall increases, C_ε decreases, becomes almost constant then increases again as the outer limit of the boundary layer is approached. Caution is certainly required when commenting on the values of C_ε in the near-wall region ($0 \leq y/\delta \leq 0.05$) and in the very outer layer ($0.8 \leq y/\delta \leq 1$) because of the unreliability of $\bar{\varepsilon}_{iso}$ to represent $\bar{\varepsilon}$ in these regions. [1] reported a similar trend in their smooth wall channel flow. However, there is a marked difference between these rough wall results and those of [1] (and [7, 6, 3] as shown in [1]). The magnitude of C_ε in the channel for $0.3 \leq y/h \leq 07$ (h is the channel half-width) is close to 1, which is about twice as large as the present value in the region $0.4 \leq y/\delta \leq 0.8$. The present value is more alingned with that for in HIT. It is not clear why there is such a difference between the channel flow and either the rough wall boundary layer or the HIT. [1] argued that the difference with the HIT is likely to be associated with the existence of large-scale u structures in the outer region, since L/h exhibits a nearly parabolic distribution with a tendency to plateau (~ 1). Figure 5 shows the distributions of L/δ across the present rough wall boundary layer. L increases as the distance from the wall increases, reaches a maximum of about 0.6δ around $y/\delta \simeq 0.2$ then decreases slowly; notice the apparent plateau in the region $0.5 \leq y/\delta \leq 0.8$, which coincides with the region over which C_ε is almost constant (see figure 4).

Using phenomenology argument ([12]), one can show that $C_\varepsilon \simeq 1/\kappa$ in the logarithmic region of the smooth wall turbulent boundary layer; κ is the von Karman constant. Assuming $\kappa \sim 0.41$ then $C_\varepsilon \simeq 2.4$. Clearly, this is not observed here, where a value close to 1 is more adequate.This may be related to the fact that the near wall dynamics on the fully rough wall differs significantly from that on the smooth wall. It may also

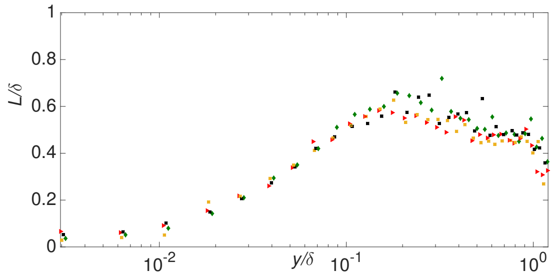

Figure 5: Distribution of L/δ as function of y/δ for various Re_θ; symbols same as in Figure 4. A semi-log scale is used to highligh the near-wall region.

be due in part to the dampening of the viscous effects in the near wall region.

Of interest is the relatively good collapse of the C_ε-distributions in the region $0.05 \leq y/\delta$, which would suggest a Reynolds number independency. This is consistent with the possibility that C_ε approaches a universal value as the Reynolds number increases to large values.

Finally, we report in Figure 6 the distribution of L/λ as function of y/δ for several Re_θ. The ratio varies significantly across the layer: as the distance from the wall increases, the ratio increases, reaches a maximum at $y/\delta \sim 0.1$, then decreases. The ratio increases systematically with Re_θ, reflecting the increase of Re_λ. It is interesting to note that the ratio in the region $0.03 \leq y/\delta \leq 0.8$ is larger than about 8, which indicates that there may be enough scale separation between the large energy containing structures and the small dissipative structures for local isotropy to hold, further providing support for the use of ε_{iso} as a surrogate for ε. Although not shown here, it was verified that $C_\varepsilon = 15(L/\lambda)/Re_\lambda = \bar{\varepsilon}_{iso}L/u'^3$, as it should be, providing a self-consistency check for C_ε.

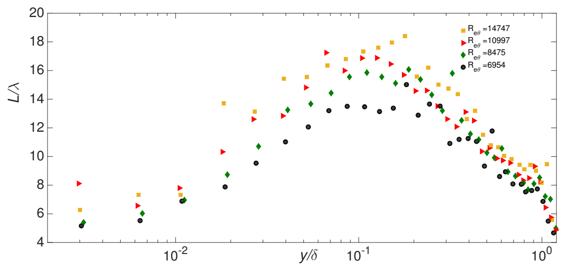

Figure 6: Distributions of L/λ as function of y/δ for various Re_θ; symbols same as in Figure 4. A semi-log scale is used to highlight the near-wall region.

Concluding remarks

Hot-wire measurements have been carried out in a fully rough wall turbulent boundary layer with the aim to assess the dependence of $C_\varepsilon = \bar{\varepsilon}L/u'^3$ on the distance from the wall and the Reynolds number. It is found that C_ε decreases as the distance from the wall increases and reaches a minimum value of about 0.4-0.5, which is the about value obtained in homogeneous isotropic turbulence at high Reynolds numbers. Further, this value appears to be Reynolds number independent, lending support to the possibility that C_ε may tend to a universal value at sufficiently large Reynolds numbers.

A word of caution is however need with regard to the present estimation of $\bar{\varepsilon}$. Since the true $\bar{\varepsilon}$ is not available, we have used $\bar{\varepsilon}_{iso}$, the locally isotropic form of ε. While this cannot be correct in the near-wall region, we expect $\bar{\varepsilon}_{iso}$ to approach the true $\bar{\varepsilon}$ in the region $0.2 \leq y/\delta \leq 0.8$ with reasonably a small uncertainty because of the relatively large values of Re_λ achieved in this region. Of course further study is required where the actual $\bar{\varepsilon}$ can be measured. At this stage, only direct numerical simulations are capable of providing such information, at least for turbulent channel flows.

Acknowledgements

The Australian Research Council (ARC) is gratefully acknowledged for the financial support of this work.

References

[1] Abe, H. and Antonia, R. A, Scaling of normalized mean energy and scalar dissipation rates in a turbulent channel flow *Phys. Fluids*, **23**, 2011,055104.

[2] Antonia, R.A., Bisset, D. K. and Browne, L. W. B. (1990) Effect of Reynolds number on the topology of the organized motion in a turbulent boundary layer. *J Fluid Mech*, **213**, 1990, 267–286.

[3] Comte-Bellot, G., Contribution a l'etude de la turbulence de conduite, *PhD. thesis*, University of Grenoble, France, 1963 (Trans. P. Bradshaw ARC 31 609 FM 4102, 1969).

[4] Djenidi, L. and Antonia, R. A., A spectral chart method for estimating the mean turbulent kinetic energy dissipation rate, *Exp.Fluids*, 2012, **53**, 1005-1013.

[5] Doering, C. and Foias, C., Energy dissipation in body-forced turbulence, *J. Fluid Mech*, **467**, 2002, 289–306.

[6] Hoyas, S. and Jimenez, J., Reynolds number effects on the Reynolds-stress budgets in turbulent channels, *Phys. Fluids*, 2008, **20**, 101511.

[7] Hu, Z. W., Morfey, C. L. and Sandham, N. D., Wall pressure and shear stress spectra from direct numerical of channel flow, *AIAA J.*, 2006, **44**, 1541–1549.

[8] Kamruzzaman, Md, Djenidi, L., Antonia, R. A. and Talluru, K. M. Drag of a turbulent boundary layer with transverse 2D circular rods on the wall, *Exp. Fluids*, **56**, 2015, 1–8.

[9] Kaneda, Y., Ishihara, T., Yokokawa, M., Itakura, K. and Uni, A., Energy dissipation rate and energy spectrum in high resolution direct numerical simulations of turbulence in a periodic box. *Phys. Fluids*, **15**, 2003, L21.

[10] McComb, W. D., *Homogeneous, Isotropic Turbulence, Phenomenology, Renormalization and Statistical Closures*. Oxford UniversityPress., 2014.

[11] McComb, W. D., Berera, A., Yoffe, S. R. and Linkmann, M. F., Energy transfer and dissipation in forced isotropic turbulence. *Phys. Rev. E*, **91**, 2015, 043013.

[12] McKeon, B. J. and Morisson, J.F., Asymptotic scaling in turbulent pipe flow, *Philos. Trans. R. Soc.* London, Ser. A, **365**, 2007, 771–787.

[13] Pearson, B., Krogstad, P.-A. and van de Water, W., Measurements of the turbulent energy dissipation rate, *Phys. Fluids*, **14**, 2002, 1288–1290.

[14] Smalley, R. J., Antonia, R. A. and Djenidi, L, Self-preservation of rough-wall turbulent boundary layers, *Eur. J. Mech. (B/Fluids)*, **20**, 2001, 591–602.

[15] Sreenivasan, K. R., The energy dissipation in turbulent shear flows, in *Symp. Development in Fluid Dynamics and Aerospace Engineering*, editors S. M. Deshpande, A. Prabhu, K. R. Sreenivasan and P. R. Viswanath, Interline Publishers, Bangalore, India, 1995, 159–190.

[16] Talluru, K. M., Djenidi, L., Kamruzzaman, Md. and Antonia, R. A., Self-preservation in a zero pressure gradient rough-wall turbulent boundary layer, *J. Fluid Mech.*, **788**, 2016, 57–69.

[17] Tennekes, H. and Lumley, J. L. *A first course in turbulence*. MIT Press, 1972, Cambridge, MA.

[18] Vassilicos, J. C, Dissipation in turbulent flows, *Annu. Rev. Fluid Mech.*, **47**, 2015, 95–114.